This is a pre-print of an article published in *Applied Biochemistry and Biotechnology*. The final authenticated version is available online at: https://doi.org/10.1007/s12010-015-1496-3

Expression and characterization of a recombinant psychrophilic Cu/Zn Superoxide Dismutase from *Deschampsia antarctica*

Juan A. Rojas-Contreras, Ana P. Barba de la Rosa, Antonio De León-Rodríguez*

División de Biología Molecular, Instituto Potosino de Investigación Científica y Tecnológica, A.C. (IPICyT), Camino a la Presa San José 2055, Lomas 4a. Sección, CP 78216, San Luis Potosí, Mexico.

Submitted to: *Appl Biochem Biotechnol*

*Corresponding author. Tel.: +52-444-8342044; fax: +52-444-8342010.

E-mail address: aleonr@ipicyt.edu.mx, aleonr@me.com

Abstract

We present the structural modeling and biochemical characterization of a recombinant Superoxide dismutase (SOD) from *Deschampsia antarctica* E. Desv. produced in *Escherichia coli*. The recombinant protein was purified by affinity chromatography Ni-NTA and its identity was demonstrated by immunoblotting and inhibition by H_2O_2, and KCN. ICP-OES analysis confirmed the presence of Cu and Zn. Modeling of the DaSOD aminoacid sequence using SWISS MODEL, and 2q2IB monomer of the psychrophilic Cu/Zu-SOD from *Potentilla atrosanguinea* as template produced a structure similar to that the typical eukaryotic Cu/Zn-SODs. Activity assays using the NBT solution method showed that the purified *D. antarctica* Cu/Zn-SOD (DaSOD) had a specific activity of 5,818 U/mg at 25°C and pH 7.2, and it was active in a pH interval of 5-8 and a temperature interval of 0-40°C. Furthermore, DaSOD was still active at -20°C as observed by a zymogram assay. We found 100% activity when it was heated at 80°C for 60 min, indicating a high thermo-stability. DaSOD properties suggest that this enzyme could be useful for preventing the oxidation of refrigerated or frozen foods, as well as in the preparation of cosmetic and pharmaceutical products.

Keywords: Antioxidant, extremophile, oxidative stress, psychrophilic enzyme, superoxide ion.

1. Introduction

Deschampsia antarctica E. Desv. is one of the only two native vascular plants living in Antarctica (5). Due to the conditions of its habitat including frozen ground, ice/snow cover, deficient precipitation, incidence of low illumination during the winter and high UV radiation during summer, high levels of reactive oxygen species (ROS) are produced, and therefore as a response, high levels of peroxidase, glutathione reductase, and superoxide dismutase (SOD) activities are present in this plant (15).

Superoxide dismutase is the first line of defense against ROS. SOD converts the superoxide anion to molecular oxygen and hydrogen peroxide (8). There are four types of SODs, and each one has a distinct metal ion in its active site: Mn, Fe, Ni, or Cu/Zn (1, 21). Eukaryotic Cu/Zn-SODs are highly conserved from primary to quaternary structure, and they are composed of two identical subunits. Each has a β-barrel of 8 antiparallel β-chains forming a Greek key motif (17). SODs are used in the preparation of a large variety of cosmetic and health-promoting supplements (3, 7, 14); therefore, the search for SODs whose properties allow better performance is of high biotechnological valuable.

In this work, we report the structural modeling and biochemical characterization of a recombinant Cu/Zn-SOD from *D. antarctica* (DaSOD) expressed in *Escherichia coli*. Structural modeling was performed using SWISS MODEL and a psychrophilic Cu/Zu-SOD from *Potentilla atrosanguinea* as template (11). The recombinant protein was purified by affinity chromatography and its activity was assessed.

2. Materials and methods

2.1 In silico modeling

The three-dimensional structure of the DaSOD was performed using the aminoacid sequence (access number ACV65038.1) and the comparative protein modeling PROTEIN SWISS MODEL server (http://swissmodel.expasy.org/), using the 2Q2L_B monomer (access number ACB38158.1) belonging to the *Potentilla atrosanguinea* Cu/Zn-SOD (11) as template.

2.2 Strain and culture media

E. coli BL21-SI (Gibco) was transformed with the plasmid pDaSOD containing the *DaSOD-His*$_6$ gene under control of the T7 promoter. A detailed description of the molecular vehicle used, concentration of trace elements in culture medium, and procedures for strain preservation and inoculum preparation can be found elsewhere (9). The production medium contained 5 g/L glucose, 3.5 g/L $(NH_4)_2HPO_4$, 3.5 g/L KH_2PO_4, 1.0 g/L MgSO4, 40 µg/L thiamine, 35 mg/L kanamycin (Sigma), and trace elements. Before autoclaving, the pH of the medium was adjusted to 7.4 with 10N NaOH. Preinocula were grown overnight in 100 mL of the production medium plus 5 g/L yeast extract (Difco). Flasks were incubated in a shaker at 250 rpm and 37°C.

2.3. Protein expression

Batch cultures were performed in a 1.3-L bioreactor (Applikon) equipped with two six-blade Rushton turbines and stirred at 300 rpm. The cultures were started with 1-L of production medium at an initial optical density at 600 nm (OD_{600nm}) of 0.2. The batch cultures were performed at 37°C until an OD_{600nm} of 0.6 was attained. Then, the expression was induced with 0.3 M NaCl and the post-induction temperature was changed to 32.5°C. The pH was maintained at 7.0 by automatic addition of a 2N NaOH solution and dissolved oxygen at 20% using an ADI-1030 Bio-controller (Applikon) and the BioXpert v1.3 software (Applikon).

2.4 DaSOD purification

Culture samples collected from the bioreactor were harvested by centrifugation at 16,000*g* for 2 min at 4°C, resuspended in 0.1M phosphate buffer pH 7.8 (PBS), and sonicated in an Ultrasonic processor GE 505 (Sonics, Newtown, CT) using 10 pulses of 10 s at 25% amplitude and 10 s resting between pulses. The soluble fraction was recovered by centrifugation at 8,000*g* for 15 min at 4°C. Protein purification was carried out using nickel-nitrilotriacetic acid (Ni-NTA) affinity columns with the ProBond Purification System (Invitrogen) following manufacturer instructions. Protein eluted was dialysate in a 10 mM Tris-HCl buffer pH 7.5 using an Amicon cell (Millipore) with ultrafiltration membranes Ultracel YM-10 (Millipore) for 3 h at 4°C.

2.5 Analytical procedures

104 Proteins were separated in 4-20% gradient sodium dodecyl sulphate polyacrylamide gel
105 electrophoresis (SDS-PAGE) using a Miniprotean III System (BioRad). Proteins were
106 visualized with Coomassie Blue R-250 (BioRad) for the bioreactor production analysis or
107 Silver stain (BioRad) after the purification process. For Western blot, proteins were
108 transferred from gel onto a nitrocellulose membrane (Amersham Biosciences, Piscataway,
109 NJ) using a Semi-Dry Transblot (BioRad). The membrane was blocked with low-fat
110 powder milk (3%, w/v in PBS). The membrane was incubated with the mouse anti-His tag
111 monoclonal antibody 0.2 µg/mL (AbD serotec, Oxford, UK), followed by goat anti-mouse
112 IgG antibody conjugated to alkaline phosphatase 1:3000 (BioRad), and visualized with *p*-
113 nitro blue tetrazolium chloride and 5-bromo-4-chloro-3-indolyl-phosphate (NBT/BCIP,
114 Amersham Biosciences). Analysis of gels and nitrocellulose membranes was carried out
115 using a photo-documenter Gel-Doc 2000 (BioRad) and the Quantity One™ v4.5 software
116 (BioRad).

117

118 *2.6 Metal quantification*

119 The metal content in the purified DaSOD was analyzed in an inductively coupled plasma
120 optical emission spectrometer (ICP-OES) Varian 730 (Palo Alto, CA).

121

122 *2.7 DaSOD activity*

123 DaSOD activity was visualized by the polyacrylamide method of Beauchamp and
124 Fridovich (4) as follows: 3 µg of purified protein was electrophoresed by a 4-20% SDS-

PAGE. The electrophoresis was carried out at 4ºC and 100 V for 4 h. Then, the gels were washed twice at room temperature with 50 mL of 10 mM Tris-HCl buffer (pH 7.9) containing 25% (v/v) of isopropanol for 25 min. The gels were incubated 25 min in 50 mM phosphate buffer (pH 7.8) containing 2.5 mM NBT, washed briefly, and incubated 15 min with 25 mL of 50 mM PBS (pH 7.8) with 1.1 mM riboflavin (Sigma, St. Louis, MO) and 1.4 mM TEMED (Sigma). Gels were washed 3 times with milliQ water and exposed to 50W white-light source (Phillips, IN) until bands were visualized. Bovine erythrocyte SOD (Sigma) was used as a control to show the activity. DaSOD activity was tested against 10 mM KCN and 5 mM H_2O_2 using zymograms. The specific DaSOD activity was measured by the free solution method of McCord and Fridovich (13). In brief, 3 mL of reaction buffer contained 13 mM L-methionine, 0.1 mM EDTA, 75 mM NBT in 50 mM PBS (pH 7.8), and 3 µL-purified enzyme o 3 µL of water as control. At time zero, 2 mM riboflavin was added and exposed to a 3800-4000 µCd LED white-light source (Steren) located 3 cm above from a 3 mL cuvette. Reduction of NBT was monitored for 10 min at 560 nm using a Spectrophotometer Cary BIO-50 (Varian, Palo Alto, CA) coupled with a cell-holder Peltier (Varian, Palo Alto, CA) with agitation and temperature control. Measurements were taken in triplicate and the average was used for results analysis. One Unit of activity was defined as the amount of enzyme needed to attain half of the maximum inhibition of NBT reduction (13).

2.8 Effect of temperature, pH, and thermo-stability

To determine the effect of temperature on the activity of the DaSOD, 5 µL aliquots of the

purified enzyme were subjected to temperatures from 0 to 70°C with increments of 10°C during the activity assay. The effect of pH was determined after incubating 5 µL aliquot of the purified DaSOD in 145 µL of various buffers with a pH range from 2 to 10, for a period of 12 h. The buffers contained, respectively: 50 mM KCl/HCl (pH 2), 50 mM glycine/HCl (pH 3), 50 mM CH_3COOH/CH_3COONa (pH 4.5), 50 mM KH_2PO_4/NaOH (pH 6-8), and glycine/NaOH (pH 9-10). Thermo-stability was determined after incubating 5 µL of the enzyme at temperatures from 80 to 110°C by intervals of 10°C for 60 min and by increments of 10 min in a Peltier thermal plate (BioRad). The relative activity of the enzyme subjected to the different treatments was determined by the free solution method described above.

3. Results and discussion

3.1 In silico modeling

DaSOD aminoacid sequence was submitted to SWISS MODEL server for modeling using automatic mode. The program constructed a tertiary structure using the 2Q2L_B biological unit as a template, which has a percentage identity of 82.237%, with the DaSOD. This suggests its tertiary and quaternary structure is similar to that of the template (Fig. 1). The 2Q2L_B unit belongs to one of the monomers of a Cu/Zn-SOD of the *Potentilla atrosanguinea* plant induced by low temperatures (20). This issue is interesting because *P. atrosanguinea* is a plant that grows in the western Himalayas, India, under extreme environmental conditions of high UV and low temperatures, similar to those supported by *D. antarctica* in the South Pole. Additionally, we performed an ANOLEA (Atomic Non-

169 Local Environment Assessment) diagram, which calculated the favorable energy of the
170 predicted structure, to give reliability to the model (6). As shown in Fig. 2, the key
171 structural elements of the DaSOD activity were located in similar areas as PaSOD. The
172 predicted DaSOD structure is similar to other Cu/Zn-SODs, which have a dimer structure
173 comprising by two identical subunits. Each monomer contains an eight-barrel chain with
174 seven loops (16). The structural differences between DaSOD and PaSOD are the disulfide
175 loops and Greek key (Fig. 1).

176

177 *3.2 Expression, immunodetection and purification of the recombinant DaSOD*

178 DaSOD was produced in batch cultures, and the maximum protein production was reached
179 at 4 h of culture after induction with 0.3 M NaCl (data not shown). Identification of
180 recombinant DaSOD after purification is shown in Fig. 3. Recombinant DaSOD was
181 purified through a column of Ni-NTA affinity under stringent conditions to prevent binding
182 of contaminating proteins as indicated by the supplier. Western-blot analysis was
183 performed using a monoclonal antibody against the His_6-tag. The assay detected a single
184 band of 16 kDa corresponding to the fused DaSOD-His_6 demonstrating the identity of the
185 DaSOD (Fig. 3a). The purity of the DaSOD was determined by densitometry analysis of a
186 SDS-PAGE with silver staining, showing that the protein had at least 97% purity (Fig. 3b).

187

188 *3.3 Biochemical characterization of the DaSOD*

DaSOD assays in solution using 5 mM H_2O_2 or 10 mM KCN fully inhibited the enzyme activity, supporting the notion of DaSOD belonging to the Cu/Zn-SOD family (data not shown). To corroborate the content of metal ions in the DaSOD, metal content was determined by inductively coupled plasma optical emission spectroscopy (ICP-OES). The analysis showed that the DaSOD contains Cu and Zn in an amount of 0.1072 and 0.1791 μg-atom/$mg_{protein}$, respectively, confirming that it is a Cu and Zn-dependent metalloprotein.

The enzymatic characterization of the DaSOD is summarized in Fig. 4 to 7. The enzyme activity was measured over a pH range of 2 to 10. As shown in Fig. 4, the enzyme was unaffected by pH in the range of 5 to 8, whereas a drop of the activity was observed above pH 8. The interval of pH-insensibly depends on the protein origin. For instance, the black soybean Cu/Zn-SOD had maximum activity between 6 and 8 (19), whereas tomato Cu/Zn-SOD had an optimal pH of 7.8 (12). As seen in Fig. 5, the optimum reaction temperature of DaSOD is between 10° and 30°C with a maximum observed at 25°C, which decreases as the temperature increases from 40° to 70°C. It is noteworthy that the enzyme had only a 20% reduction of the maximal activity when incubated at 0°C and having detectable activity when assessed at -20°C in SDS-PAGE as reported by Garcia-Echauri *et al.* (9). These data clearly indicate that the DaSOD belongs to a very small group of SODs active at cold temperatures (0°C) (22), and the second of its kind active at -20°C (18). The thermal-stability of DaSOD was investigated by incubating at 80°C, 90°C, 100°C, and 110°C, respectively. The results showed that DaSOD was not affected at 80°C, and the half-life time was 35 min at 100°C, whereas at 110°C, the enzyme was completely inactivated in 20 min (Fig. 6). A hyper-thermostable SOD isolated from a polyextremophile higher plant *Potentilla atrosanguinea* was engineered by mutation of a single amino acid that enhanced

212 the thermo-stability of the enzyme twofold (11).

213 Under optimal conditions, the purified DaSOD had a specific activity of 5,818 U/mg at
214 25°C and pH 7.2. As seen in Fig. 7, the inhibition percentage of NBT photoreduction assay
215 was not linear with the concentration of DaSOD, showing a typical Michaelis-Menten
216 behavior. Under the conditions of our assay and using the equation of Asada *et al.* (10, 2),
217 the K´ that is a function of the concentration of NBT and determines the affinities of
218 DaSOD and NBT on the superoxide anion was 0.1719 µg/mL (10, 2).

219

220 **4. Conclusions**

221 We present the structural modeling and biochemical characterization of a recombinant
222 Superoxide dismutase (SOD) from *Deschampsia antarctica* E. Desv. produced in
223 *Escherichia coli.* DaSOD exhibits some properties similar to those of most plant Cu/Zn-
224 SODs, such as molecular weight, thermal stability, and pH stability. However, DaSOD
225 shows activity under freezing conditions and high thermo resistance. DaSOD properties
226 suggest that this enzyme could be useful for preventing the oxidation of refrigerated or
227 frozen foods, as well as in the preparation of cosmetic and pharmaceutical products.

228

229 **Acknowledgements**

230 We acknowledge that this work has been partially supported by CONACyT-Básicas Grant
231 No. 178988. Juan Rojas thanks CONACyT for scholarship No. 204213. The authors thank
232 Leandro G. Ordoñez for technical support and Jennifer Ecklerly for English correction.

233

References

1. Alscher, R. G., Erturk, N. and Heath, L. S. (2002) Role of superoxide dismutases (SODs) in controlling oxidative stress in plants. J Exp Bot, **53,** 1331-1341.
2. Asada, K., Takahashi, M. and Nagate, M. (1974) Assay and inhibitors of spinach superoxide dismutase. AGric. Biol. Chem., **38,** 471-473.
3. Bafana, A., Dutt, S., Kumar, S. and Ahuja, P. S. (2011) Superoxide dismutase: an industrial perspective. Crit Rev Biotechnol, **31,** 65-76.
4. Beauchamp, C. and Fridovich, I. (1971) Superoxide dismutase: improved assays and an assay applicable to acrylamide gels. Analytical biochemistry, **44,** 276-287.
5. Bravo, L. A., Ulloa, N., Zuniga, G. E., Casanova, A., Corcuera, L. J. and Alberdi, M. (2001) Cold resistance in Antarctic angiosperms. Physiol Plantarum, **111,** 55-65.
6. Chodanowski, P., Grosdidier, A., Feytmans, E. and Michielin, O. (2008) Local Alignment Refinement Using Structural Assessment. Plos One, **3,** e2645.
7. Di Mambro, V. M. and Fonseca, M. J. (2007) Assessment of physical and antioxidant activity stability, in vitro release and in vivo efficacy of formulations added with superoxide dismutase alone or in association with alpha-tocopherol. European journal of pharmaceutics and biopharmaceutics: official journal of Arbeitsgemeinschaft fur Pharmazeutische Verfahrenstechnik e.V, **66,** 451-459.
8. Fridovich, I. (1997) Superoxide anion radical (O^{-2} radical anion), superoxide dismutases, and related matters. J Biol Chem, **272,** 18515-18517.
9. Garcia-Echauri, S. A., Gidekel, M., Moraga, A. G., Ordonez, L. G., Contreras, J. A. R., Barba de la Rosa, A. P. and De Leon Rodriguez, A. (2009) Heterologous expression of

a novel psychrophilic Cu/Zn superoxide dismutase from Deschampsia antarctica. Process Biochem, **44,** 969-974.

10. Giannopolitis, C. N. and Ries, S. K. (1977) Superoxide dismutases: I. Occurrence in higher plants. Plant physiology, **59,** 309-314.
11. Kumar, A., Dutt, S., Bagler, G., Ahuja, P. S. and Kumar, S. (2012) Engineering a thermo-stable superoxide dismutase functional at sub-zero to >50^{o} C, which also tolerates autoclaving. Scientific reports, **2,** 387.
12. Kumar, S., Dhillon, S., Singh, D. and Singh, R. (2004) Partial purification and characterization of superoxide dismutase from tomato (lycopersicon esculentum) fruit. J Food Sci Nutr, **9,** 283-288.
13. McCord, J. M. and Fridovich, I. (1969) Superoxide dismutase. An enzymic function for erythrocuprein (hemocuprein). J Biol Chem, **244,** 6049-6055.
14. Mizushima, Y., Hoshi, K., Yanagawa, A. and Takano, K. (1991) Topical application of superoxide dismutase cream. Drugs under experimental and clinical research, **17,** 127-131.
15. Perez-Torres, E., Garcia, A., Dinamarca, J., Alberdi, M., Gutierrez, A., Gidekel, M., Ivanov, A. G., Huner, N. P. A., Corcuera, L. J. and Bravo, L. A. (2004) The role of photochemical quenching and antioxidants in photoprotection of Deschampsia antarctica. Funct Plant Biol, **31,** 731-741.
16. Perry, J. J. P., Shin, D. S., Getzoff, E. D. and Tainer, J. A. (2010) The structural biochemistry of the superoxide dismutases. Bba-Proteins Proteom, **1804,** 245-262.
17. Richardson, J. S. (1977) beta-Sheet topology and the relatedness of proteins. Nature, **268,** 495-500.

18. Sahoo, R., Kumar, S. and Ahuja, P. S. (2001) Induction of a new isozyme of superoxide dismutase at low temperature in Potentilla astrisanguinea Lodd. variety argyrophylla (Wall. ex. Lehm) Griers. J Plant Physiol, **158,** 1093-1097.

19. Wang, S. Y., Shao, B., Liu, S. T., Ye, X. Y. and Rao, P. F. (2012) Purification and characterization of Cu, Zn-superoxide dismutase from black soybean. Food Res Int, **47,** 374-379.

20. Yogavel, M., Gill, J., Mishra, P. C. and Sharma, A. (2007) SAD phasing of a structure based on cocrystallized iodides using an in-house CuK alpha X-ray source: effects of data redundancy and completeness on structure solution. Acta Crystallogr D, **63,** 931-934.

21. Youn, H. D., Kim, E. J., Roe, J. H., Hah, Y. C. and Kang, S. O. (1996) A novel nickel-containing superoxide dismutase from Streptomyces spp. Biochem J, **318,** 889-896.

22. Zheng, Z., Jiang, Y. H., Miao, J. L., Wang, Q. F., Zhang, B. T. and Li, G. Y. (2006) Purification and characterization of a cold-active iron superoxide dismutase from a psychrophilic bacterium, Marinomonas sp NJ522. Biotechnol Lett, **28,** 85-88.

Figure captions

Fig. 1. Superimposition of DaSOD (green) and PaSOD (blue) obtained by SWISS MODEL. The differences found in the Greek key loops and disulfide are shown with green and blue arrows, respectively. Histidine involved in the coordination of Zn^{+2} ion is shown in yellow, histidine-bridge in orange, which coordinates both Zn^{+2} and Cu^{+2} ions. Green and blue histidines show those involved in the coordination of Cu^{+2} ion.

Fig. 2. Graphic ANOLEA showing the evaluation of the tertiary model predicted for DaSOD. Favorable and unfavorable energy regions are shown in green and red, respectively.

Fig. 3. DaSOD-His_6 identification after purification. A) SDS-PAGE analysis of protein DaSOD purified by affinity chromatography on a column of Ni-NTA agarose. Lane 1, 10 µL of sample eluted. Lane 2, molecular weight marker. B) Immunoblot of SDS-PAGE gel showed in Fig 3A. C). Analysis by SDS-PAGE of the purity of the DaSOD-His_6. 10 µL of resin and the various fractions eluted from the Ni-NTA column were electrophoresed, and the gel was stained with $AgNO_3$. Lane 1, molecular weight marker. Lane 2-5, different fractions of the protein eluted with imidazole.

Fig. 4. Effect of pH on the relative DaSOD activity measured at 20°C.

Fig. 5. Determination of optimal Temperature for de DaSOD activity measured at pH 7.2.

Fig. 6. Thermo-resistance assay of the DaSOD activity measured at pH 7.2.

Fig. 7. Inhibition of NBT photoreduction assay against increasing concentration of purified DaSOD. The assays were performed at pH 7.2 and 20°C.

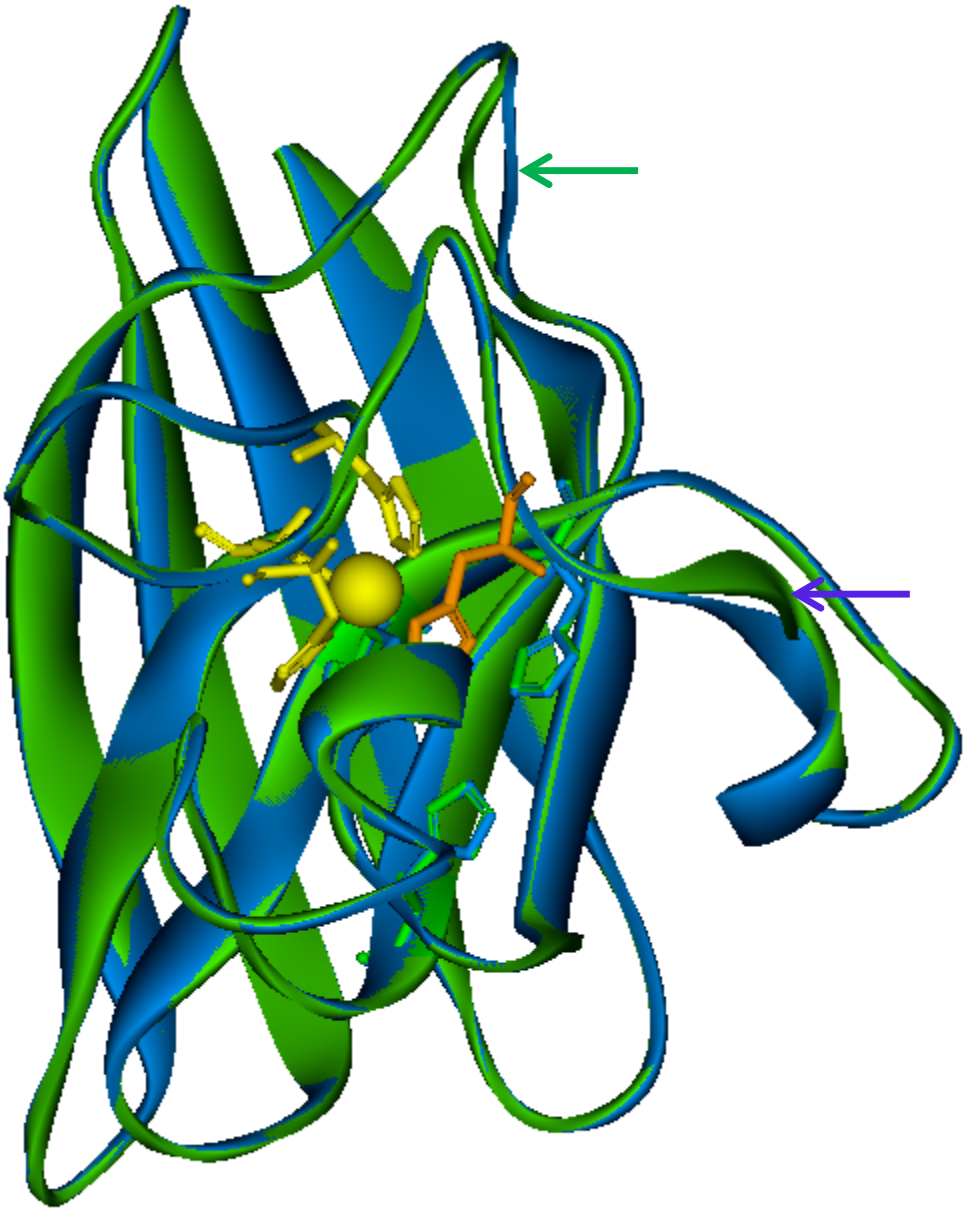

Fig. 1.

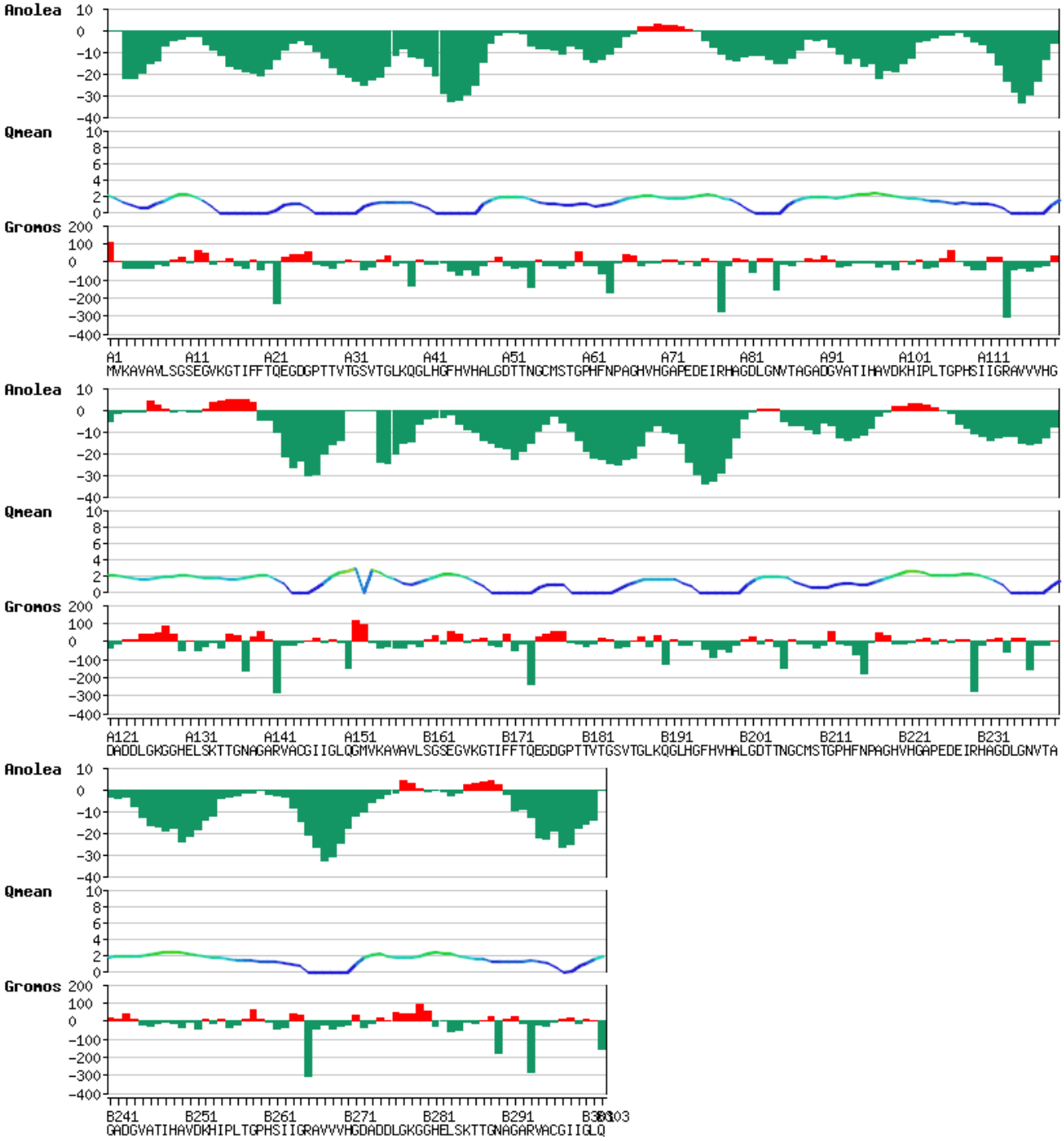
Anolea
Qmean
Gromos
A1 A11 A21 A31 A41 A51 A61 A71 A81 A91 A101 A111
MVKAVAVLSGSEGVKGTIFFTQEGDGPTTVTGSVTGLKQGLHGFHVHALGDTTNGCMSTGPHFNPAGHVHGAPEDEIRHAGDLGNVTAGADGVATIHAVDKHIPLTGPHSIIGRAVVVHG
Anolea
Qmean
Gromos
A121 A131 A141 A151 B161 B171 B181 B191 B201 B211 B221 B231
DADDLGKGGHELSKTTGNAGARVACGIIGLQGMVKAVAVLSGSEGVKGTIFFTQEGDGPTTVTGSVTGLKQGLHGFHVHALGDTTNGCMSTGPHFNPAGHVHGAPEDEIRHAGDLGNVTA
Anolea
Qmean
Gromos
B241 B251 B261 B271 B281 B291 B303
GADGVATIHAVDKHIPLTGPHSIIGRAVVVHGDADDLGKGGHELSKTTGNAGARVACGIIGLQ

Fig. 2.

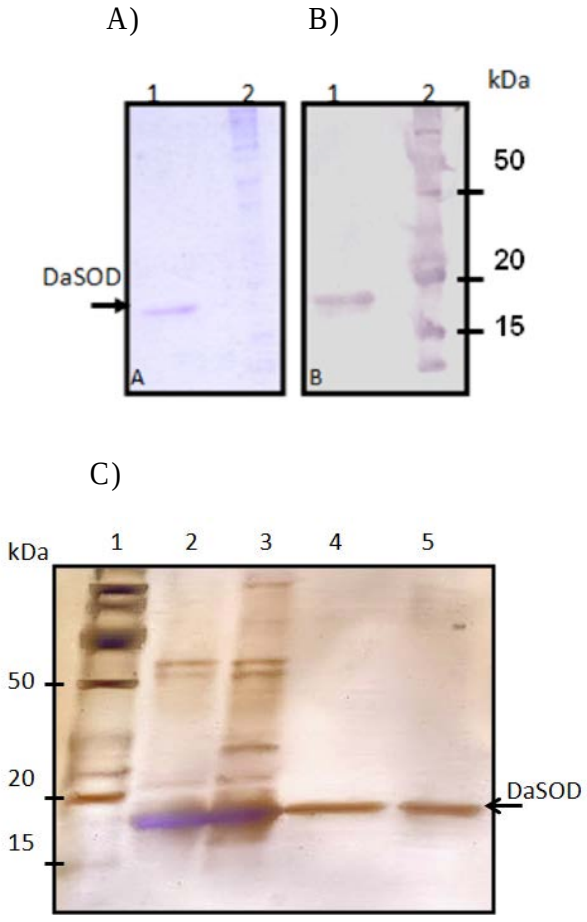

Fig. 3

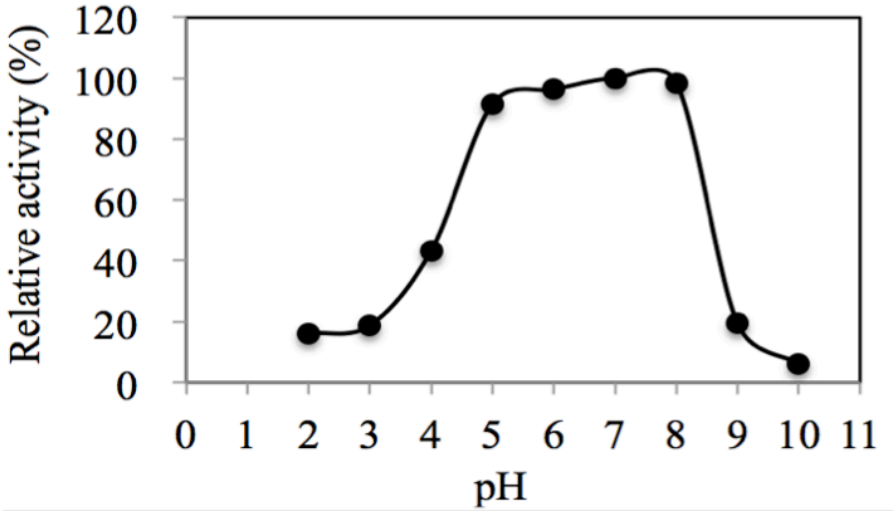

Fig. 4.

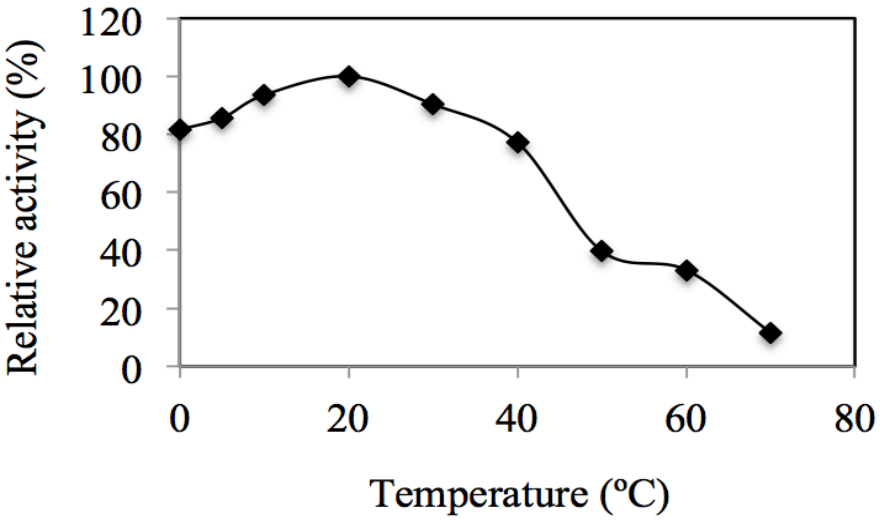
Relative activity (%)
120
100
80
60
40
20
0
0
20
40
60
80
Temperature (ºC)

Fig. 5.

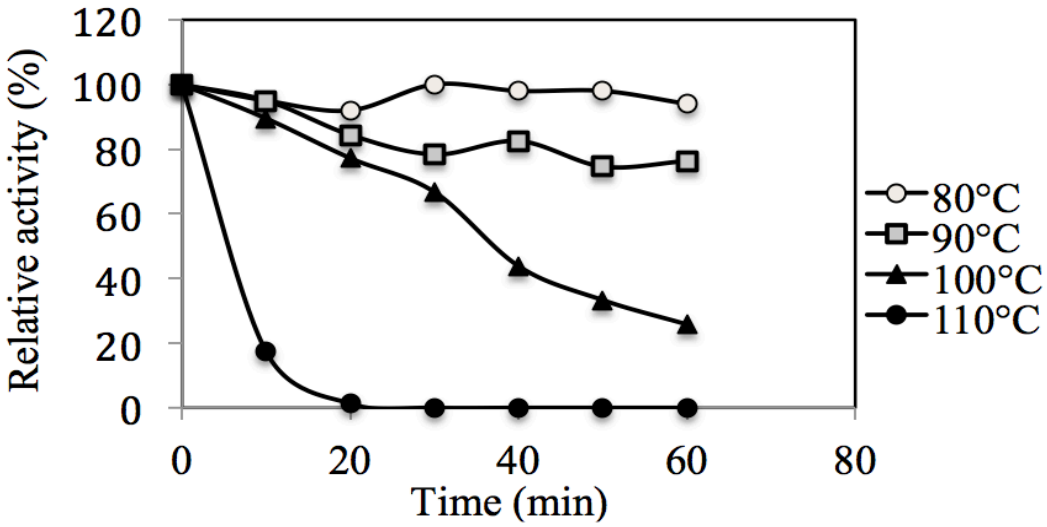
120
100
80
60
40
20
0
Relative activity (%)
0
20
40
60
80
Time (min)
80°C
90°C
100°C
110°C

Fig. 6.

403

404

405

406

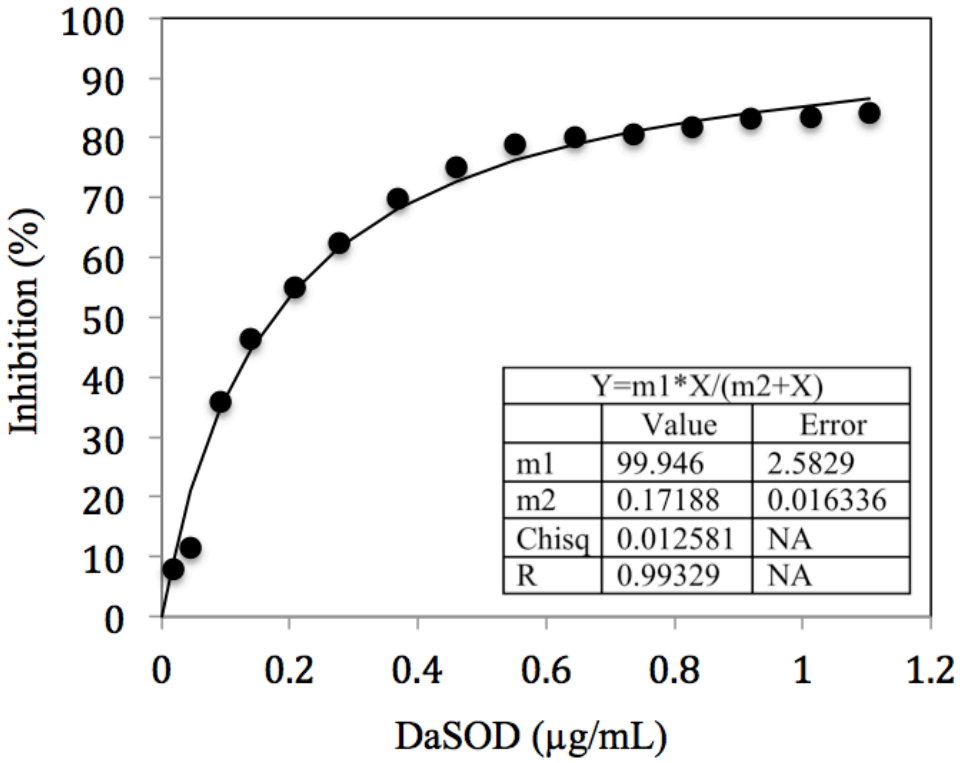

407

408 Fig. 7